

Observed Regimes of Mid-Latitude and Tropical Cirrus Microphysical Behavior

A. D. Del Genio and A. B. Wolf
National Aeronautics Space Administration
Goddard Institute for Space Studies
New York, New York

G. G. Mace
University of Utah
Salt Lake City, Utah

L. M. Miloshevich
National Center for Atmospheric Research
Boulder, Colorado

Introduction

Little is known about the climatological microphysical properties of cirrus clouds. Thus, general circulation model (GCM) cirrus parameterizations often assume either constant effective radius (r_e) or constant crystal number concentration N (Del Genio et al. 1996). The net feedback effect of cirrus in a climate change can be either warming or cooling depending on how cirrus properties change, so there is a clear need to develop physically-based parameterizations rooted in observations. The Atmospheric Radiation Measurement (ARM) Program Millimeter Wave Cloud Radars (MMCRs) at the Southern Great Plains (SGP) and Tropical West Pacific (TWP) sites offer the opportunity to collect climatically significant statistics of cirrus properties in different seasons and different climate regimes. We use retrievals based on the algorithm of Mace et al. (1998) to explore the properties of SGP cirrus during November 1996 - May 1998 and of TWP (Nauru) cirrus during the period January 1999 - November 2000. Figure 1 shows log-log plots of retrieved cirrus crystal r_e vs. ice water content (IWC) for (upper left) the Goddard Institute for Space Studies GCM, showing the $r_e \propto (\text{IWC})^{1/3}$ behavior that results when N is assumed constant; (lower left) the TWP, showing two populations of clouds, one with large particles for which r_e is independent of IWC with much scatter, and a second group of small particles in which r_e decreases with increasing IWC; (upper right) the SGP in summer, showing a hint of the latter behavior at the TWP plus another population of clouds for which r_e increases with IWC; (lower right) the SGP in winter, showing only r_e increasing with IWC. Clearly real-world behavior differs markedly from either $r_e = \text{constant}$ or $N = \text{constant}$.

Anecdotal evidence for processes controlling the different populations of clouds comes from examining the large-scale morphology of the clouds. Based on the previous figure, we divided the TWP dataset into large- and small-particle subsets, and we examined infrared satellite images acquired close in time to MMCR retrievals in the two populations. Images taken at times when large-particle cirrus existed over Nauru indicate that the sampled cirrus appear to be part of an extensive cold cloud system

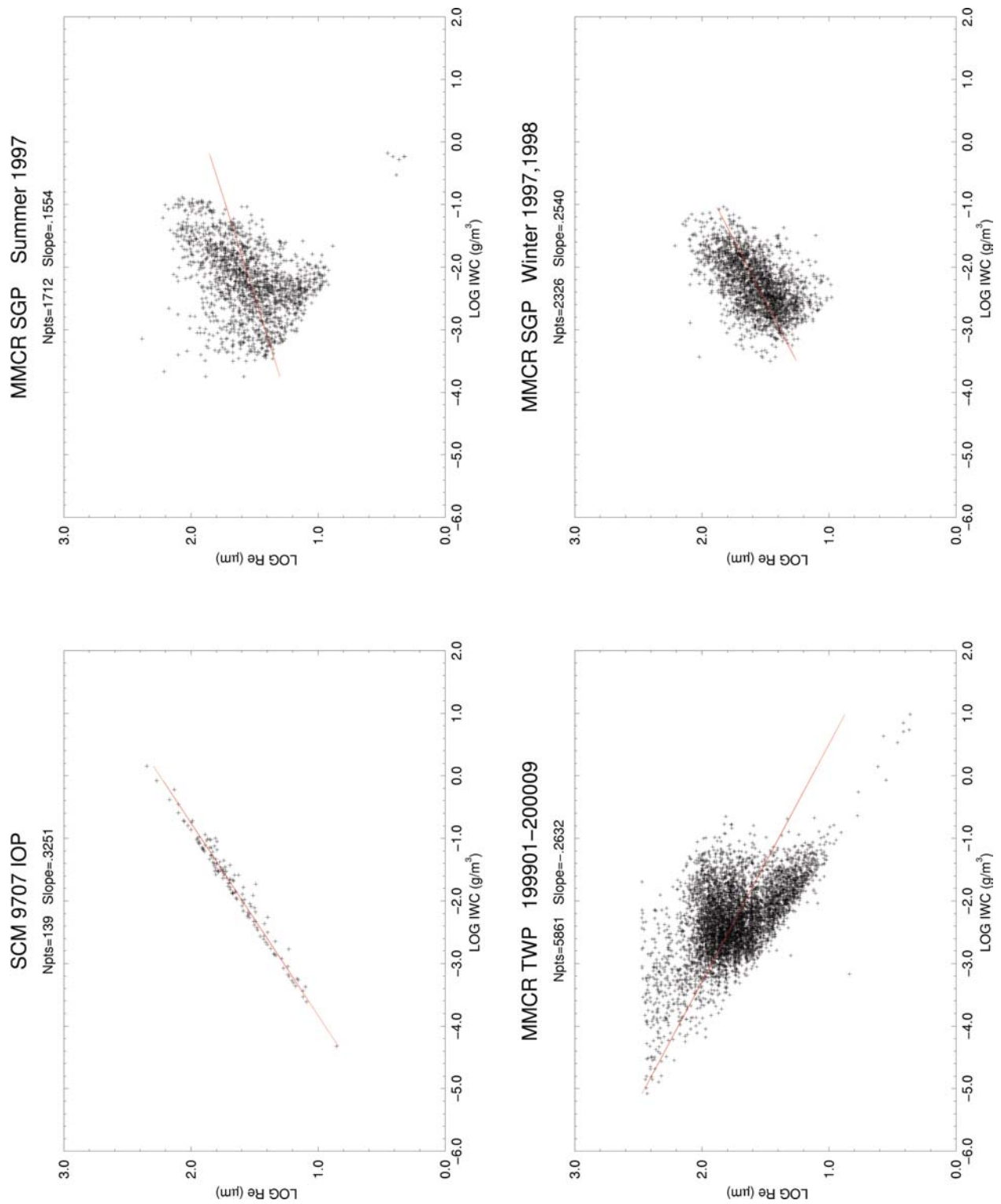


Figure 1. . Log-log plots of cirrus crystal r_e vs. IWC for (upper left) the Goddard Institute for Space Studies GCM, (lower left) the TWP Nauru site, (upper right) the SGP in summer, (lower right) the SGP in winter.

ostensibly associated with a deep convective event. This provides a ready explanation for the randomness of the r_e -IWC relationship seen in Figure 1. Detrained ice crystals originate in the planetary boundary layer from air with different levels of humidity and aerosol concentration depending on wind direction and precise altitude of parcel origin, and complex primary and secondary microphysical processes in the convective updraft can lead to a variety of particle sizes for a given amount of ice. With one exception, cirrus in the small-particle population appear to form tens to hundreds of kilometers away from the nearest convective cloud, though perhaps physically connected to the detrainment of water vapor from the nearest system. The tendency of these cloud particles to be smaller when ice contents are large may be an artifact of loss of sensitivity of the radar, since most of these clouds have very low radar reflectivities; whatever the precise nature of their microphysical properties, though, other properties of these clouds presented below suggest that they are the result of different physics than that which creates the large-particle population.

We divided the data into clouds with base temperature $< -37^\circ\text{C}$ and base temperature $> -37^\circ\text{C}$ at both sites. Clouds with warm bases exhibit a single behavior at each site, with modest values of N and a moderate rate of increase with IWC ($N \propto \text{IWC}$ for the TWP and $N \propto \text{IWC}^{1/2}$ for the SGP). Clouds with cold bases exhibit two different types of behavior at each site—some behave like their warm base counterparts, but others (corresponding to the small-particle population in Figure 1) have much higher values of N , suggesting that they are formed by the process of homogeneous nucleation, which operates efficiently only at cold temperatures.

Dividing the points into large-particle (red histograms) and small-particle (blue histograms) populations, we see (Figure 2) that the number concentrations (left panels) of large particles are about an order of magnitude greater at the SGP than at the TWP, suggesting that at least some of these clouds may form via heterogeneous nucleation on aerosols derived from the boundary layer at each site and advected to higher altitude. The SGP-TWP difference is presumably a reflection of the cleaner, more maritime air mass at the TWP as opposed to the more polluted, continental air mass at the SGP. The small particle cirrus at both sites have much higher number concentrations, with less difference between the sites. Ice water contents (right panels) of large-particle cirrus peak at small values, but somewhat greater at the TWP than the SGP. Small-particle cirrus exist almost exclusively with small IWC at the SGP but span the full range of IWC values at the TWP.

Figure 3 shows that cirrus on average tend to occur ~ 1 km higher in altitude at the TWP than at the SGP (left panels), but otherwise their characteristics are fairly similar. The large-particle population tends to have thicknesses of ~ 1 to 3 km, with the SGP clouds being slightly thicker than the TWP cirrus (right panels). The small-particle population generally exists at higher altitude at both sites, consistent with their colder temperatures, and most of them are < 1 km thick. Figure 4 shows that despite their other differences, optical thickness distributions (left panels) are fairly similar at both sites and for both large- and small-particle populations, with most clouds having optical thickness < 0.5 . This occurs because small particle sizes tend to occur in physically thin clouds, producing offsetting radiative effects. GCMs, by comparison, do not resolve cirrus thicknesses < 1 to 2 km, and their radiative properties tend to be determined by IWC alone. Few large-particle cirrus are formed with bases colder than 220 K (right panels) at either location, while almost all of the small-particle cirrus form at $T < 240$ K (-33°C), consistent with the suggested homogeneous nucleation source.

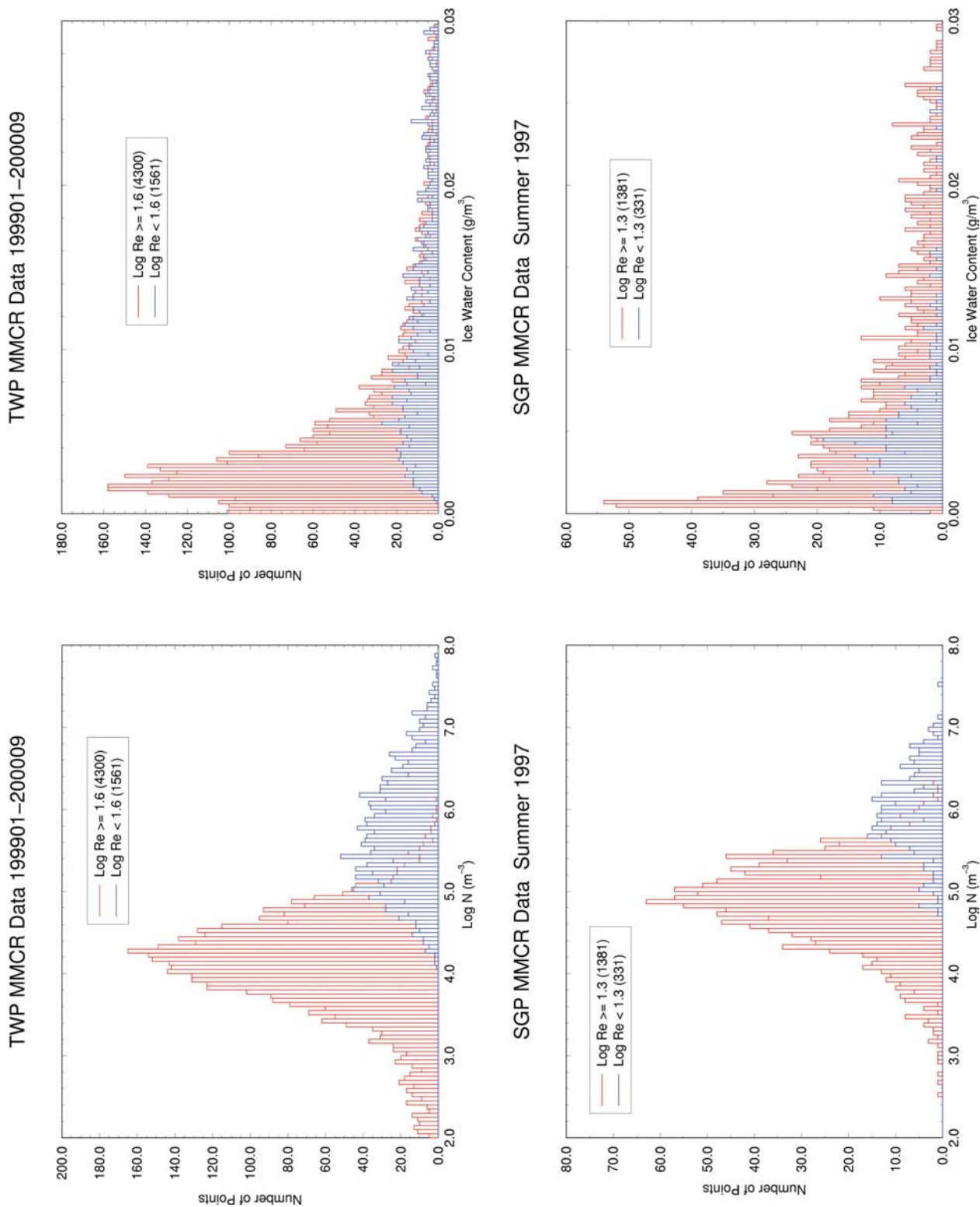


Figure 2. Histograms of cirrus properties for large-particle (red) and small particle (blue) populations (upper left) log N at the TWP, (lower left) log N at the SGP in summer, (upper right) IWC at the TWP, (lower right) IWC at the SGP in summer.

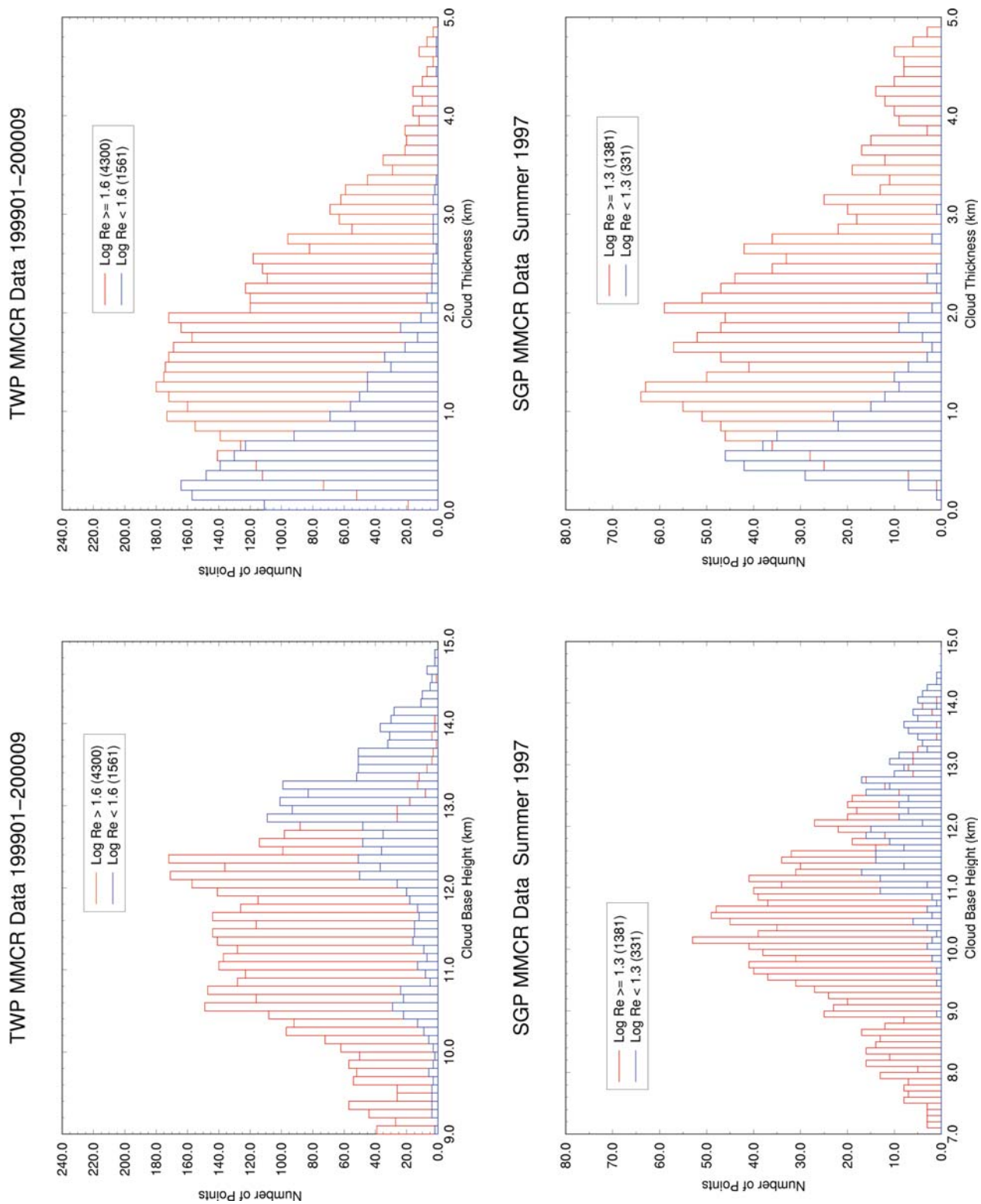


Figure 3. As in Figure 2, but for cloud base height (left) and cloud physical thickness (right).

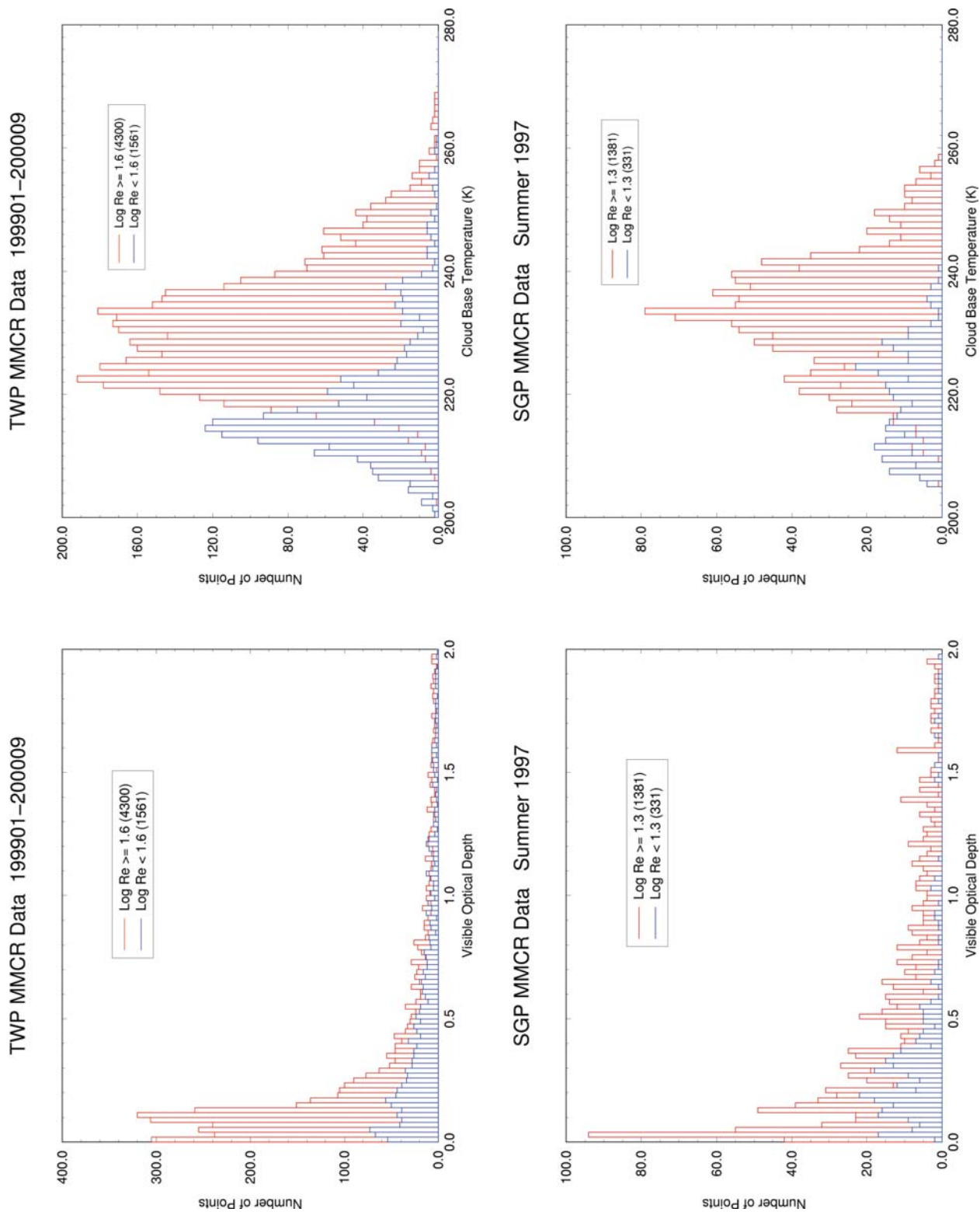


Figure 4. As in Figure 2, but for visible optical thickness (left) and cloud base temperature (right).

Sometimes cirrus are detected continuously over the sites for a sufficiently long time to observe their evolution (though we cannot tell the difference between a currently evolving but uniform cirrus and one that has evolved to a greater or lesser extent in different parts of the cloud that are advected over the radar at a given time). TWP cirrus are rarely observed for more than a couple of hours at a time, while SGP cirrus can last for many hours over the site. Within a given population, different types of evolution can be observed, but more often than not a continuous cirrus system over one of the sites changes with time in a manner consistent with the statistical behavior of the entire population. Thus, the population characteristics define both differences between individual cirrus and temporal evolution of a given cirrus cloud.

Relative humidity soundings taken within two minutes of four of the TWP small-particle cirrus events were found (Figure 5). Humidity soundings at cold temperatures have a variety of biases, and these were corrected using the technique of Miloshevich and Paukkunen (2002). The blue curves represent the original sounding, the black curves a smoothed version of the data, the green curves are the result after correction for several sonde dry-bias errors, and the red curves represent the final profiles after also correcting for sonde time-lag errors. The dashed curve represents ice saturation and the asterisk denotes the tropopause. The MMCR cirrus layers for each case reside at 13.1 to 13.2 km (upper left), 13.0 to 13.5 km (upper right), 13.0-14.4 km (lower right), and 13.6 to 14.2 km (lower right). We see that in all cases, the cirrus forms in a moist layer that extends from beneath to just above the tropopause, consistent with the idea that these clouds are at least indirectly associated with convective detrainment, albeit from a distant source. Except for the very thin cirrus case, for which the profile barely saturates, the other three examples exist in a highly ice-supersaturated layer. The degree of supersaturation is roughly consistent with the threshold relative humidity for homogeneous nucleation of solution droplets at very cold temperatures derived from parcel models of freezing point depression (Sassen and Dodd 1989) and observations of wave clouds (Heymsfield and Miloshevich 1995). Note also the presence of another ice-supersaturated layer in each sounding at warmer temperatures in which the MMCR detects no cirrus. This is consistent with the finding of the above studies that 100% relative humidity with respect to water is required to homogeneously nucleate at warm temperatures. The absence of cloud in these warmer layers argues for the unimportance of heterogeneous nucleation at these times. Heterogeneous nucleation is more likely in the larger-particle cirrus cases that occur at temperatures too warm for homogeneous nucleation to be important.

We therefore suggest a possible conceptual model for the three observed populations. (1) Small-particle physically thin cirrus at both sites dominate in the absence of significant concentrations of ice nuclei at cold temperatures, when sufficient turbulence exists to provide multiple homogeneous nucleation episodes; such clouds form from moisture detrained from convective updrafts but far away from them, so their evolution depends on the local environment. (2) Large-particle thicker cirrus layers at the SGP occur either via homogeneous or heterogeneous nucleation when turbulence is weaker, so that N increases slowly and IWC increases occur mostly via growth of existing particles in synoptic-scale updrafts; convective detrainment may be an important source of water and condensation or ice nuclei for these cirrus in summer, but even at this time the evolution of the layer is controlled by synoptic-scale processes. (3) Large-particle thicker cirrus at the TWP are a more direct result of the detrainment of ice transported upward in convective cores; they have different altitudes of origin within the boundary layer, different aerosol concentrations, and form in updrafts of different strength, leading to a random distribution of particle sizes and ice contents not directly related to conditions in the upper troposphere.

twp_delgenio

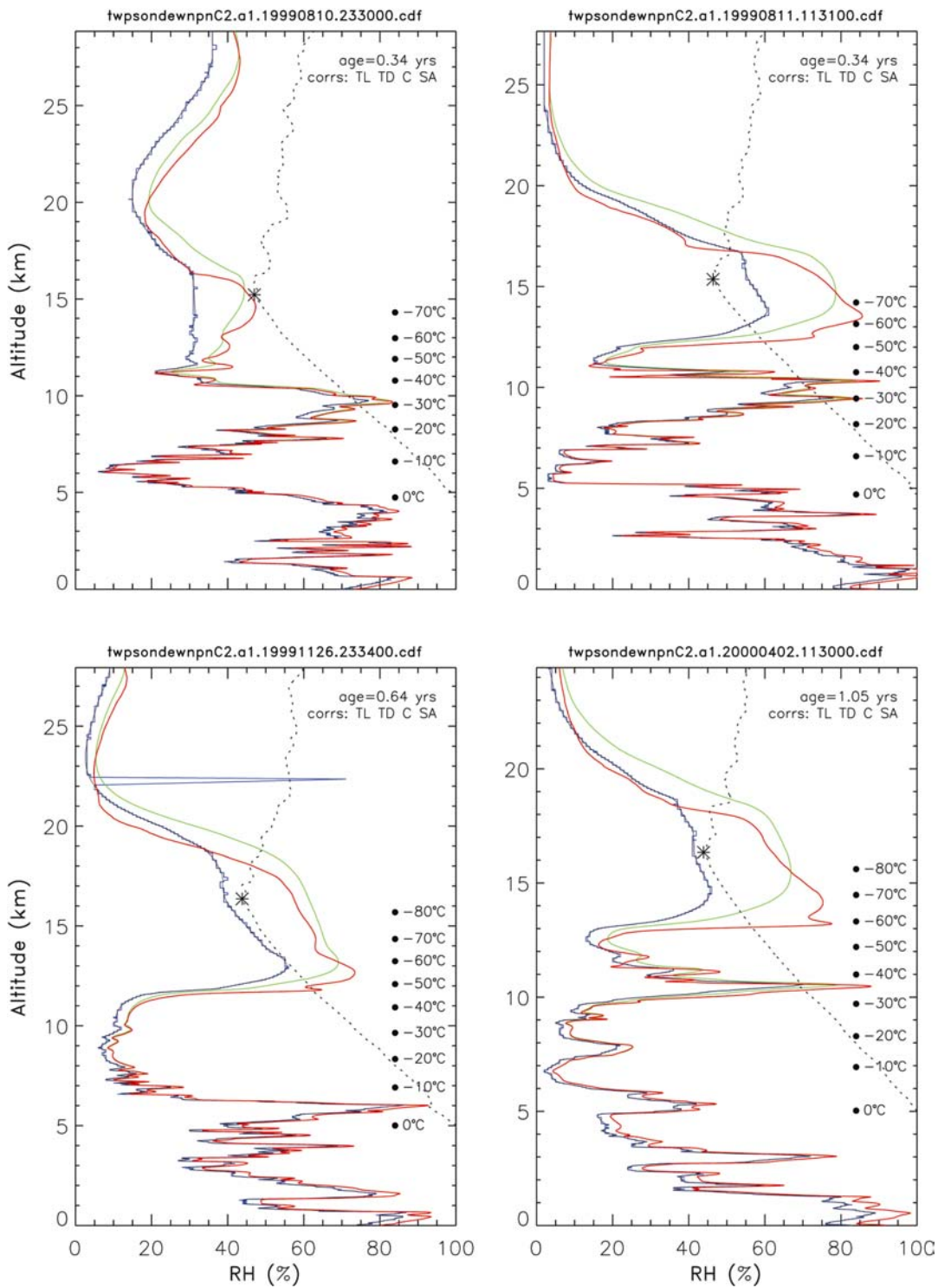


Figure 5. TWP humidity soundings corrected for cold-temperature biases for four times within 2 minutes of a near-tropopause, small-particle thin cirrus observation. The different curves are described in the text.

Once the microphysical properties of the small-particle population are determined to greater accuracy, the results presented here could form the basis of a parameterization of cirrus number concentration in climate GCMs, making possible a more accurate prediction of the contribution of cirrus clouds to climate sensitivity.

Corresponding Author

Anthony D. Del Genio, adelgenio@giss.nasa.gov, (212) 678-5588

References

Del Genio, A. D., M. -S. Yao, W. Kovari, and K.K.-W. Lo, 1996: A prognostic cloud water parameterization for global climate models. *J. Clim.*, **9**, 270-304.

Heymsfield, A. M., and L. M. Miloshevich, 1995: Relative humidity and temperature influences on cirrus formation and evolution: Observations from wave clouds and FIRE II. *J. Atmos. Sci.*, **52**, 4302-4326.

Mace, G. G., T. P. Ackerman, P. Minnis, and D. F. Young, 1998: Cirrus layer microphysical properties derived from surface-based millimeter cloud radar and infrared radiometer data. *J. Geophys. Res.*, **103**, 23,207-23,216.

Miloshevich, L. M., and A. Paukkunen, 2002: Impact of Vaisala radiosonde humidity corrections on ARM IOP data. This proceedings.

Sassen, K., and G. C. Dodd, 1989: Haze particle nucleation simulations in cirrus clouds and applications for numerical and lidar studies. *J. Atmos. Sci.*, **46**, 3005-3014.